© 2018. Published by The Company of Biologists Ltd | Journal of Cell Science (2018) 131, jcs210492. doi:10.1242/jcs.210492

RESEARCH ARTICLE

Abscisic acid – an anti-angiogenic phytohormone that modulates the phenotypical plasticity of endothelial cells and macrophages

Julienne Chaqour[1], Sangmi Lee[1], Aashreya Ravichandra[1] and Brahim Chaqour[1,2,*]

ABSTRACT

Abscisic acid (ABA) has shown anti-inflammatory and immunoregulatory properties in preclinical models of diabetes and inflammation. Herein, we studied the effects of ABA on angiogenesis, a strictly controlled process that, when dysregulated, leads to severe angiogenic disorders including vascular overgrowth, exudation, cellular inflammation and organ dysfunction. By using a 3D sprouting assay, we show that ABA effectively inhibits migration, growth and expansion of endothelial tubes without affecting cell viability. Analyses of the retinal vasculature in developing normoxic and hyperoxic mice challenged by oxygen toxicity reveal that exogenously administered ABA stunts the development and regeneration of blood vessels. In these models, ABA downregulates endothelial cell (EC)-specific growth and migratory genes, interferes with tip and stalk cell specification, and hinders the function of filopodial protrusions required for precise guidance of vascular sprouts. In addition, ABA skews macrophage polarization towards the M1 phenotype characterized by anti-angiogenic marker expression. In accordance with this, ABA treatment accelerates macrophage-induced programmed regression of fetal blood vessels. These findings reveal protective functions of ABA against neovascular growth through modulation of EC and macrophage plasticity, suggesting the potential utility of ABA as a treatment in vasoproliferative diseases.

KEY WORDS: Abscisic acid, Angiogenesis, Retina, Oxygen-induced retinopathy, Hyaloid vessel, Macrophage

INTRODUCTION

Abnormal angiogenesis is a hallmark of numerous pathologies, including vasoproliferative diseases of the eye; for example, retinopathy of prematurity (ROP), proliferative diabetic retinopathy (PDR), age-related macular degeneration, neovascular glaucoma, diabetic nephropathy, vasculatis, inflammatory bowel diseases and tumorigenesis (Battegay, 1995; Das and McGuire, 2003; Meshkani and Vakili, 2016; Yan and Chaqour, 2013). Neovascular growth in various tissue beds is characterized by the invasion of avascular areas with excessive, tortuous and disorganized blood vessels that are prone to exudation/leakage, fibrosis and various degrees of cellular inflammation. Vascular endothelial growth factor (VEGF) has been identified as a culprit pathogenic factor responsible for both the aberrant growth of blood vessels and vascular edema (Robinson and Stringer, 2001). As a result, treatment modalities have been revolutionized by anti-VEGF drugs involving either neutralization by engineered antibodies (e.g. the antigen-binding fragments Ranibizumab, Bevacizumab and Pegaptanib), chimeric receptors (e.g. Aflibercept; VEGF-Trap R1R2), or laser treatment that alleviates ischemia, a major stimulus for VEGF expression (Kimoto and Kubota, 2012; Pertl et al., 2015; Semeraro et al., 2015; Stewart, 2011; Tolentino, 2011). Although partially effective, serious adverse effects have been associated with anti-VEGF agents, including dysfunction of glomerular filtration in the kidney, bronchopulmonary dysplasia and even visual impairment due to the critical neuroprotective functions of VEGF (Brar et al., 2010; Eremina et al., 2006, 2003; Nishijima et al., 2007; Thébaud and Abman, 2007). Significant progress is still needed in angiogenic pharmacotherapy to uncover safer and efficacious therapeutic agents.

Rather than developing new synthetic drugs that non-selectively target angiogenic and non-angiogenic signaling pathways, evaluating natural phytochemicals, which generally act through multiple cell-signaling mechanisms, but minimally affect the overall health of tissues, is a better alternative approach. Abscisic acid (ABA), a phytohormone most commonly known for inhibiting germination, is an example of such a natural product. ABA, also known as dormin, plays a major role in the induction and maintenance of seed dormancy, an effect largely attributed to its anti-mitogenic effect that counteracts that of growth-stimulating hormones, such as gibberellins (Jacobsen et al., 2002). The inhibitory potential of ABA on seed germination increases plant tolerance to abiotic stresses (e.g. temperature variations, constant light exposure, osmotic stress, and water and nutrient withdrawal) (Ng et al., 2014). Recent studies have reported the synthesis and activity of ABA in lower metazoan and higher mammalian cells, and have shown a remarkable conservation of ABA signals from plants to mammals (Zocchi et al., 2001). When exposed to a physical or chemical stress, human leukocytes produce ABA, which enhances several of their functional properties, including phagocytosis (Bruzzone et al., 2012). ABA is also released by human and murine pancreatic β-cells in response to glucose (Bruzzone et al., 2008). Nanomolar concentrations of ABA stimulated glucose-dependent and -independent insulin release. Other studies with human specimens have revealed prominent anti-inflammatory properties of ABA as indicated by a marked reduction of immune cell infiltrates at the sites of inflammation (Sakthivel et al., 2016). Mechanistically, ABA either diffuses passively across biological membranes or shuttles in and out of cells by means of transport proteins including *Arabidopsis thaliana* (At)ABCG25, which is mainly expressed in plant vascular tissue (Kuromori et al., 2010). Intracellular ABA was reported to activate a signaling cascade involving the phosphorylation and activation of ADP-ribosyl cyclase, overproduction of the universal Ca^{2+} mobilizer

[1]The Department of Cell Biology, State University of New York (SUNY) Downstate Medical Center, Brooklyn, NY 11203, USA. [2]The Department of Ophthalmology, SUNY Downstate Medical Center, Brooklyn, NY 11203, USA.

*Author for correspondence (bchaqour@downstate.edu)

J.C., 0000-0003-1086-0955; A.R., 0000-0001-5785-8524; B.C., 0000-0002-8516-4324

Received 1 September 2017; Accepted 19 December 2017

Journal of Cell Science (2018) 131, jcs210492. doi:10.1242/jcs.210492

cyclic ADP-ribose (Bruzzone et al., 2007), and the increase of the intracellular concentration of cyclic AMP or Ca^{2+} (Zhu et al., 2007). Transduction of these signals culminates into the expression of numerous stress-responsive genes, some of which are common in both plant and animal cell signaling (Ng et al., 2014). Of particular interest, ABA was found to upregulate the peroxisome proliferator-activated receptor γ (PPARγ) both *in vitro* and *in vivo* (Guri et al., 2008; Hontecillas et al., 2013). By targeting PPARγ, as the thiazolidinedione classes of anti-diabetic drugs do, ABA has the potential to ameliorate the symptoms of inflammatory diseases.

The identification of these novel properties of ABA has provided the rationale basis for further studies to explore and expand the clinical usefulness of ABA in the treatment of inflammation-induced vasoproliferative disorders. The current study was designed to determine the effects of ABA on physiological and pathological angiogenesis using both *in vitro* and *in vivo* models of vascular sprouting and neovascular diseases. Our studies identified, for the first time, the anti-angiogenic properties of ABA and showed that this phytohormone acts largely by altering the phenotypical plasticity of endothelial cells (ECs) and skewing the canonical polarized inflammatory statuses of macrophages toward an anti-angiogenic phenotype (the proportion with the M1 phenotype as opposed to the pro-angiogenic M2 phenotype).

RESULTS

ABA inhibits endothelial cell sprouting in a 3D angiogenesis model

Sprouting angiogenesis requires several distinct but cooperative mechanisms, some of which can be recapitulated by using EC-coated cytodex microcarrier beads embedded into a fibrin gel (Nakatsu et al., 2003). This model recapitulates EC sprouting, migration, alignment, proliferation, tube formation, branching and anastomosis. To determine the effects of ABA on EC sprouting, EC-coated cytodex beads were embedded into fibrin gels and incubated in increasing concentrations of ABA. The number and length of sprouts per bead were microscopically assessed after 2 and 6 days in culture. Angiogenic sprouts led by endothelial tip cells with filopodial extensions emerged from the beads on day 2 (Fig. 1A). EC sprouts were tailed by tube-like structures that started to anastomose. ECs continued to proliferate, migrate, branch and form a complex network at day 6. However, exposure to ABA dose-dependently reduced EC budding (Fig. 1B). At 1 µM concentration, only a few sprouts emerged from the microcarrier beads, and these migrated a shorter distance in the fibrin gel after 2 days. After 6 days, ECs that emerged from the cytodex beads were detached from one another and failed to anastomose. At higher concentrations (e.g. 10 and 100 µM), EC budding was completely inhibited as most ECs remained attached to the beads. The effects of ABA on EC

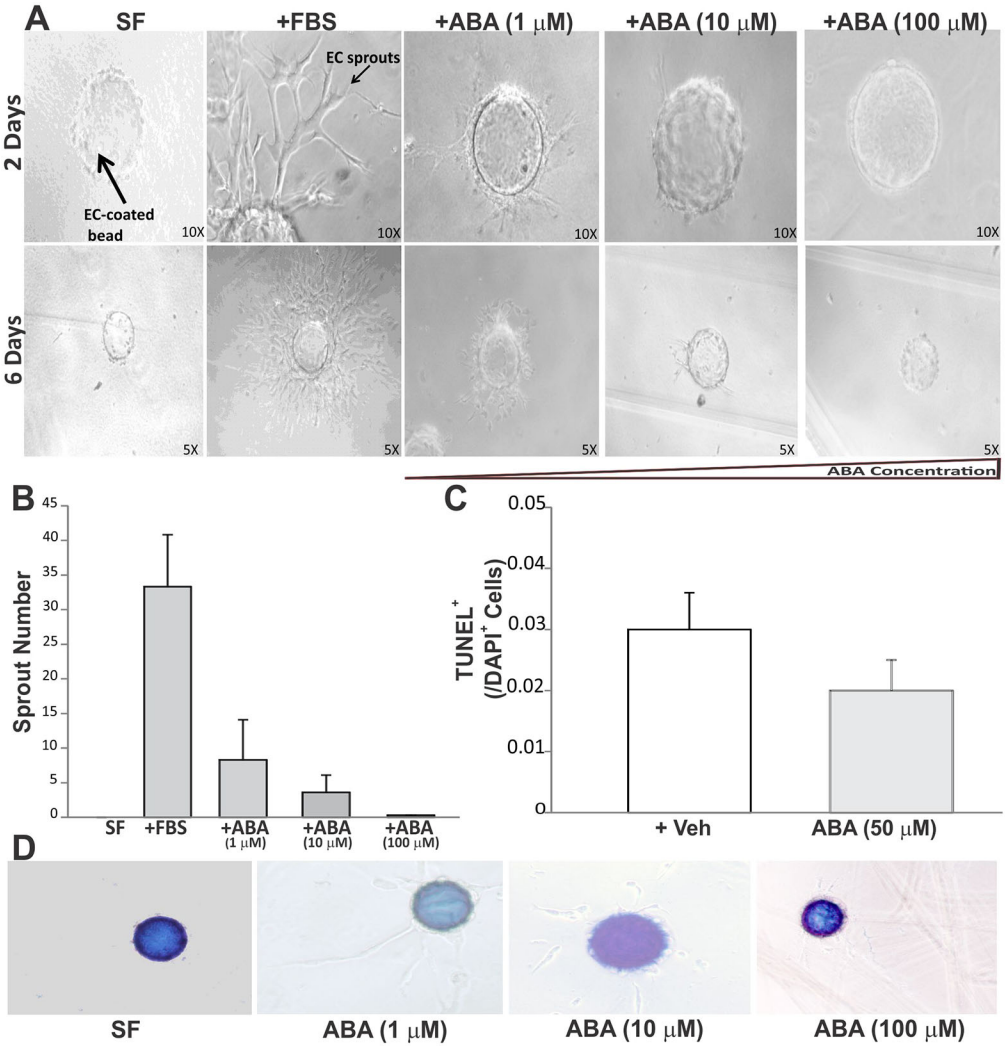

Fig. 1. Effects of ABA on retinal EC capillary-like tube formation in a fibrin gel. (A) Retinal EC-coated cytodex beads were incubated for 1 day in serum-free (SF) or fetal bovine serum (FBS)-containing medium with increasing concentrations of ABA. Angiogenic sprout formation was assessed through the visualization of fibrin gel-embedded beads at days 2 and 6. For scale, beads are 100–150 mm diameter. (B) The number of sprouts per ABA treatment group was determined. Values are the mean±s.e.m. number of sprouts per bead in at least three microwells. (C) Effect of ABA treatment on EC apoptosis. Quantification of TUNEL-positive ECs following treatment with either SF medium containing vehicle (i.e. DMSO) alone or ABA. Data are presented as mean±s.e.m. (n=3). (D) Effects of ABA on EC viability during capillary tube formation in fibrin gel. EC-coated beads were prepared and incubated as described in A and further incubated with Trypan Blue for 2 min. Cells excluding the dye from their cytoplasm are viable.

Journal of Cell Science (2018) 131, jcs210492. doi:10.1242/jcs.210492

apoptosis and viability were assessed by using terminal deoxynucleotidyl transferase dUTP nick end labeling (TUNEL) and Trypan Blue exclusion assays, respectively. As shown in Fig. 1C,D, ABA treatment did not affect the number of TUNEL-positive cells in culture. Similarly, cells treated with different concentrations of ABA remained viable with an intact plasma membrane excluding the dye from the cytoplasm. Thus, ABA had no cytotoxic effect on cultured ECs.

Effects of ABA on angiogenic sprouting during postnatal vascular development in the mouse retina

We used the postnatal mouse retina, a convenient, easily accessible and directly observable model of *in vivo* angiogenesis, to determine the effects of ABA on vascular sprouting and expansion *in vivo*. At postnatal day (P)1, a superficial layer of vessels emerged from the optic nerve head, and extended across the retinal surface spreading steadily to reach the edge of the retina at P8 (Fig. 2A). As blood vessels form, some remodel into arteries, capillaries and veins, while others grow radially towards the deeper layers of the retina. In this model, ABA was injected intravitreally at P2 and the vascular phenotype was assessed at P4 and P7. As shown in Fig. 2B,C, the superficial capillary plexus expanded progressively and effectively in eyes injected with the vehicle alone, reaching the retinal periphery by P7. However, expansion of the retinal vasculature was delayed in ABA-injected eyes. ABA did not induce vaso-obliteration but significantly reduced the spreading of the capillary plexus by 15% of the distance from the optic nerve head to the retinal edge. EC growth as determined by measuring 5-bromo-2-deoxyuridine (BrdU) incorporation within a 300–400 µm radius behind the vascular front, was significantly reduced following ABA treatment as compared to what was observed with the vehicle alone. TUNEL-positive cells were not detected in the retinal vascular plexus of ABA-treated eyes (Fig. 2E,F). However, apoptotic cells were readily detected in the outer nuclear layer (ONL) of retinas from vehicle-treated eyes and their number decreased, although not significantly, following ABA treatment. In addition, vascular

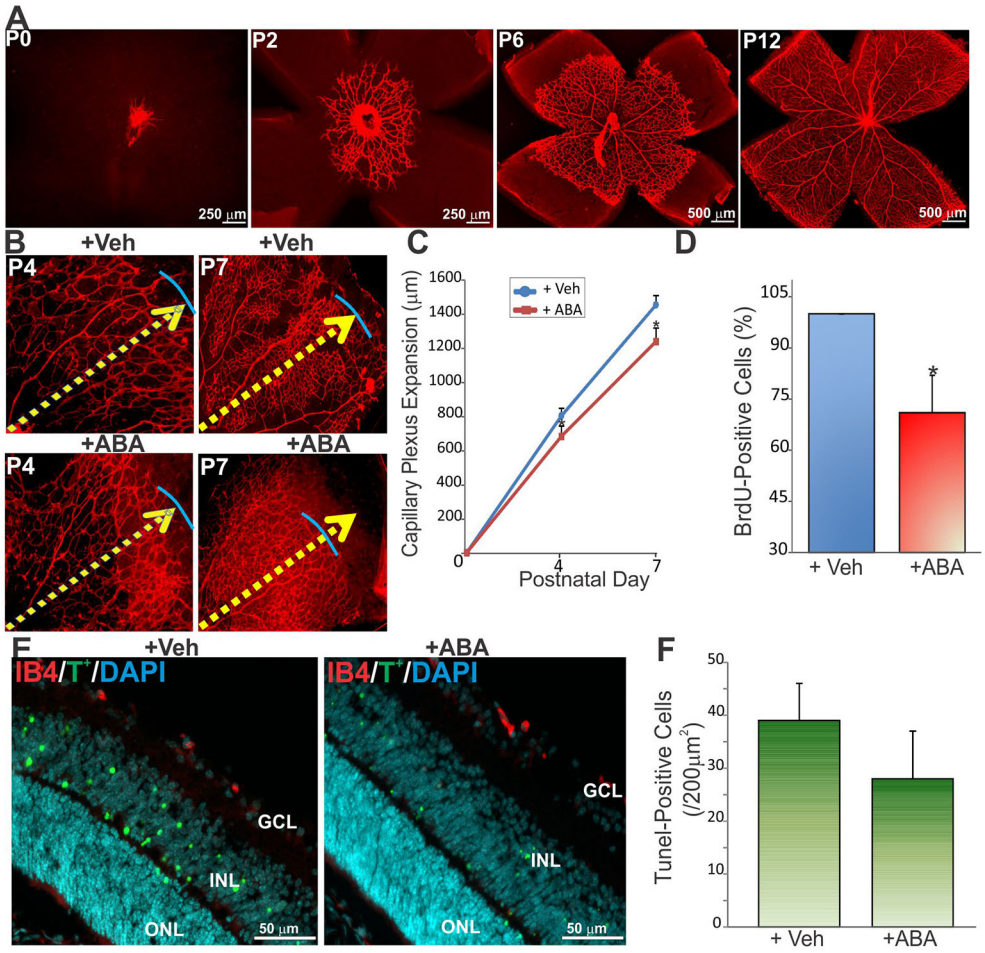

Fig. 2. The dynamic nature of retinal capillary plexus development in new born mice in the presence and absence of ABA. (A) Development of blood vessels as seen in a centrifugal spread from the optic nerve head in flat-mounted preparations of mouse retinas at P0, P2, P6 and P12. Retinas were from mouse pups raised in room air under normal light and temperature conditions and stained with isolectin B4 (IB4). (B) Intravitreal injection of ABA (50 µM) delayed the expansion of the superficial capillary plexus to the retinal edge. Mouse pups were intravitreously injected at P2 with either ABA or vehicle (Veh) and retinal flat mounts were prepared at P4 and stained with IB4. Arrows highlight the normal expansion of retinal vessels from the optic nerve head to the vascular front. (C) Capillary plexus expansion from the optic nerve head to the vascular front was measured following ABA or Veh injection at P4 and P7. *P<0.05 versus +Veh at the same postnatal day. (D) Quantitative analysis of vascular cell proliferation at P6 in the retinal vascular front of mice after intravitreous injection of ABA or Veh. The number of BrdU-positive nuclei was used as an index of cell growth in IB4-stained blood vessels. Equivalent areas of retinas from eyes injected with ABA and Veh were compared. Data are means±s.e.m. (n=5). *P<0.05 versus +Veh. (E) TUNEL staining (green) in Veh- and ABA-treated mouse retinal sections. The eyes were treated with either vehicle or ABA (50 µM) and analyzed after 48 h. Sections were counterstained with IB4 (red). Nuclei staining (blue), DAPI. GCL, ganglion cell layer; INL, inner nuclear layer. (F) Quantification of TUNEL-positive cells in retinal sections (n=6 for each group). Data are presented as mean±s.e.m. (n=6).

Journal of Cell Science (2018) 131, jcs210492. doi:10.1242/jcs.210492

perfusion and permeability were determined in vehicle- and ABA-treated mice 2 min after retroorbital injection of FITC–albumin. The injected fluorescent reporter labeled the retinal vascular plexus uniformly and remained confined within the perfused IB4-stained vasculature (Fig. S1). Thus, ABA administration suppressed vascular cell proliferation, and reduced vascular sprouting and expansion, but neither cell death nor vascular integrity was affected.

ABA inhibits tip ECs migration and proliferation

Vessel sprouting is initiated when ECs differentiate into tip cells (Fig. 3A), which define the direction of new sprout growth and create new connections between different sprouts to generate an interconnected and functional vascular network (Chaqour, 2013; Krupska et al., 2015). Intravitreal injection of ABA resulted in the alteration of tip cell shape and morphology. In ABA-treated eyes, tip cells appeared thinner with fewer filopodial extensions and their number was reduced by 30% (Fig. 3B–D). EC differentiation into tip cells is based on the activity of Dll4–Notch signaling, which promotes an adequate ratio of tip and stalk cells by suppressing tip cell formation in adjacent cells. In vehicle-treated eyes, Dll4 immunostaining was largely localized in tip cells and to a lesser extent in adjacent stalk cells at the advancing front of the vascular edge (Fig. 3E). Following ABA treatment, the Dll4 signal was highly visible in tip and stalk cells at the edge of the growing plexus. ABA treatment induced a fivefold increase in the Dll4 signal in ECs at the vascular front, indicating increased Notch1 activation in angiogenic ECs. Blocking Notch activation with a γ-secretase inhibitor, reversed, at least in part, the ABA effects, allowing a near normalization of the number of tip cells and a subsequent reduction of the formation of enlarged blood vessels due to Notch inhibitor-induced overproliferation of ECs (Fig. S2). This partial rescue of Notch inhibition by ABA may be due to the fact that Notch is not the only substrate of γ-secretase and the Notch inhibitor acts on all cell types (Koch et al., 2008). ABA treatment, at least in part, phenocopied Notch1 gain of function, which decreases the number of ECs that acquire the tip cell phenotype (Hellström et al., 2007). In addition, the expression of glial fibrillary acidic protein (GFAP) commonly known as a marker of retinal stress (Mervin and Stone, 2002), was not altered by ABA (Fig. S3A). Conversely, ABA treatment significantly reduced the expression of the *CTGF* gene, commonly associated with the angiogenic phenotype of ECs (Fig. S3B). Thus, not only does ABA treatment inhibit the motility/migratory phenotype of ECs, but it also interferes with their differentiation.

Effects of ABA on pathological angiogenesis in the retina

The mouse model of oxygen-induced retinopathy (OIR) (i.e. 75% oxygen from P7–P12 to induce vasoobliteration, and normoxia until P17 to produce maximal preretinal neovascularization) recapitulates the features of severe ROP in preterm infants and PDR in human adults (Hartnett, 2015). The retinopathy response associated with the hyperoxic insult results in the excessive and aberrant outgrowth of retinal vessels that abnormally invade the avascular vitreous leading to retinal detachment and blindness (Kuiper et al., 2008). To assess the effects of ABA on pathological angiogenesis, we subjected mouse pups to OIR and examined the subsequent retinal vascular alterations following intravitreal injection of ABA. Exposure of mouse pups to hyperoxia from P7 to P12 resulted in the obliteration of the central superficial capillary plexus (Fig. 4A). Nearly 43% of the retinal surface was vasoobliterated in mouse pups treated with either vehicle or ABA, suggesting that ABA had no protective effects against the hyperoxic injury (Fig. 4B). At P17, preretinal neovascular tufts were abundantly formed in the central and mid-peripheral retina in mice injected with the control vehicle alone. Conversely, ABA treatment at 1 µM concentration reduced neovascular tuft formation by 21% compared to vehicle treatment. Injection of ABA at a higher concentration (50 µM) suppressed both neovascularization and revascularization of the retina (Fig. 4C–E). In many cases, neovascular tufts were undetectable on the retinal surface, which is consistent with the anti-angiogenic activity of this molecule during sprouting angiogenesis.

ABA interferes with retinal neovascularization, at least in part, by mitigating the phenotypical plasticity and migratory potential of ECs

To gain insights into the cellular and molecular processes affected by ABA treatment, we examined the morphological attributes and properties of endothelial tip cells during retinal neovascularization. A typical tip cell produces 5–12 filopodial processes during developmental angiogenesis. During the ischemic phase of OIR, there was a substantial increase in the number of filopodia per endothelial tip cell, as 70% of ECs produced more than 13 filopodia per cell (Fig. 5A,B). Conversely, less than 5% of ECs produced 13 filopodial processes, while 80% of tip cells produced less than four filopodial extensions per cell following ABA treatment. Conceivably, the loss of filopodial protrusions impedes the migratory ability of endothelial tip cells and interferes with vascular sprout formation and patterning. We further determined the expression levels of several EC-specific genes encoding promigratory proteins including roundabout 4 (Robo4), C-type lectin 14A (CLEC14A) and endothelial cell-specific chemotaxis regulator [ECSCR; also known as endothelial cell-specific molecule 2 (ECSM2)]. As shown in Fig. 5C, ABA treatment was associated with a 75% reduction of the expression of CLEC14A, a transmembrane protein that localizes predominantly in filopodial processes and promotes EC migration (Verma et al., 2010). Similarly, ABA decreased the expression of ECSCR, which is indispensable for filopodial formation, EC migration and tube formation (Mura et al., 2012). ABA did not significantly alter the expression of Robo4, an endothelium-specific transcription factor with context-dependent effects on filopodia formation (Fujiwara et al., 2006). Similarly, the expression of the endothelial transmembrane protein Unc5B, a Robo4 ligand that is highly expressed on endothelial tip cells, was not significantly altered. Thus, ABA treatment, at least partly, phenocopies knockdown of endogenous promigratory genes such as ECSCR and CLEC14A and is sufficient to promote endothelial quiescence and suppress retinal neovascularization.

ABA effects on macrophage activation and angiogenic behavior

Macrophages are one of the first cells that sense chemical and physical stresses and respond to such disturbances in almost all tissues and organs. Under pathological conditions, macrophages are recruited to the hypoxic areas and reprogrammed to produce either anti-angiogenic or angiogenic factors (i.e. the M1 or M2 phenotype, respectively). Therefore, we examined whether ABA affects macrophage recruitment and polarization during retinal neovascularization. We first evaluated the infiltration of $F4/80^{+}$ macrophages in the retina during the ischemic phase of OIR. As shown in Fig. 6A, macrophages were detected around the preretinal neovascular tufts in both vehicle- and ABA-treated mice. The macrophage count was not significantly altered upon ABA treatment, indicating that ABA did not affect macrophage

Journal of Cell Science (2018) 131, jcs210492. doi:10.1242/jcs.210492

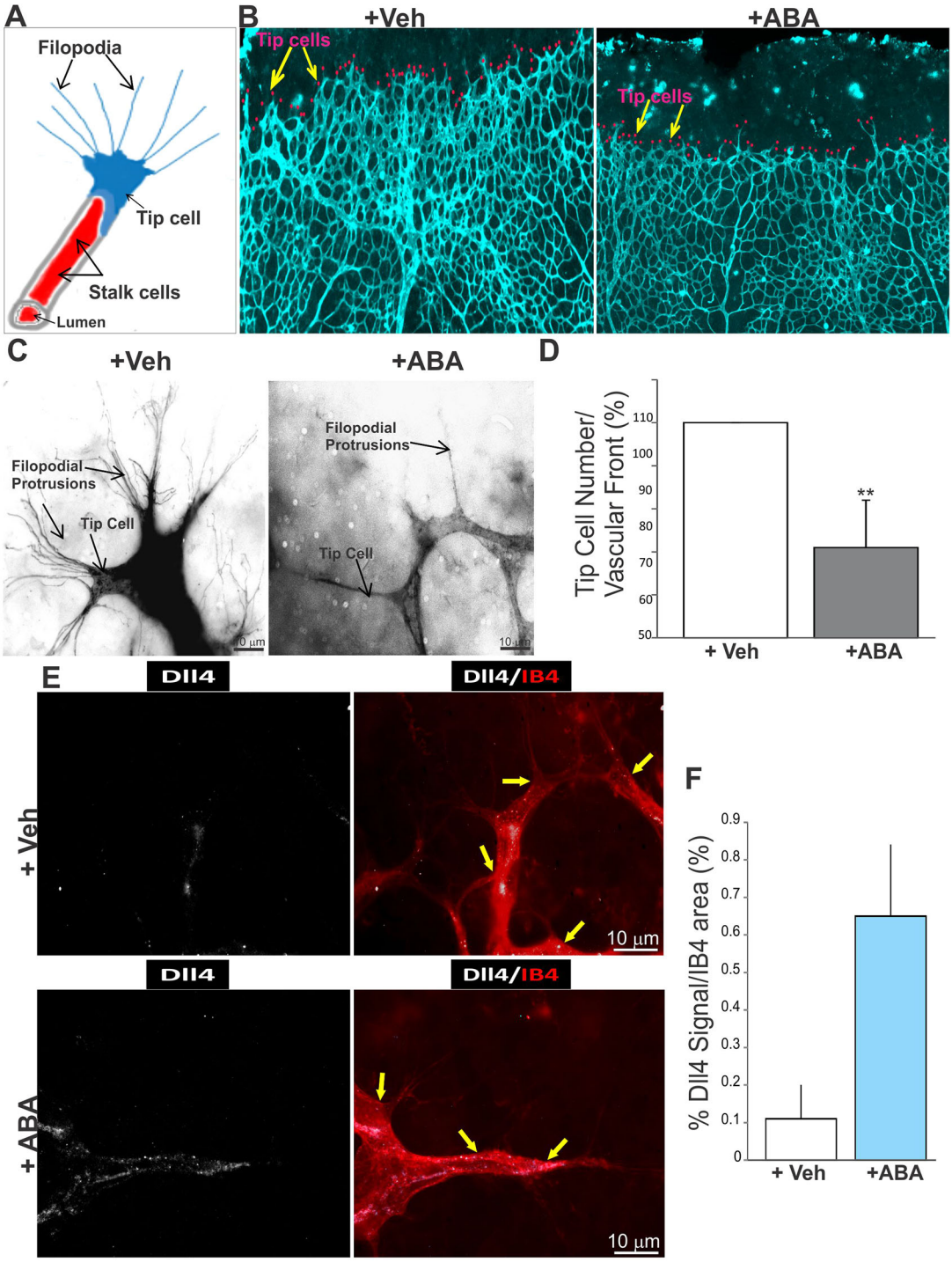

Fig. 3. ABA alter differentiation and morphology of endothelial tip cells. (A) Diagram of functional specialization of ECs into tip and stalk cells during sprouting angiogenesis. (B) Typical vascular fronts of flat-mounted IB4-stained retinas from vehicle- and ABA-injected eyes. ABA (50 µM) or vehicle was injected intravitreously to P4 mouse pups. IB4-staining was overexposed to visualize the filopodia (scored with red dots) at the vascular front. Arrows highlight tip cells. (C) High magnification view of tip ECs in the vascular front of ABA- and vehicle-injected eyes. Note the reduced number of filopodial extensions in ABA-injected eyes. (D) Quantification of filopodia-rich endothelial tip cells in the retina of ABA-injected mice and their control counterparts. Values represent means±s.e.m. (n=4). **P<0.05. Tip cells were counted in four equivalent areas of each retina. (E) Localization of Dll4 protein in ECs of the vascular edge in the retinas of P4 vehicle- and ABA-treated mice. Whole-retinal mounts were stained with IB4 (red) and for Dll4 (white punctate). Arrows indicate the tip cell locations. (F) Quantification of the percentage of Dll4+ signal normalized to the IB4+ area.

infiltration of the ischemic areas in the retina (Fig. 6B). Real-time quantitative PCR results showed that ABA treatment significantly increased the amount of OIR-induced M1 macrophage markers such as CXCL10, Socs2, Klf2 and CCN1 expression, and dampened M2 macrophage-related markers including Arg-2 and IL-4 expression (Fig. 6C,D). Since ischemia is commonly associated with increased VEGF levels, ABA treatment reduced the ischemic response by significantly reducing VEGF expression in

Journal of Cell Science (2018) 131, jcs210492. doi:10.1242/jcs.210492

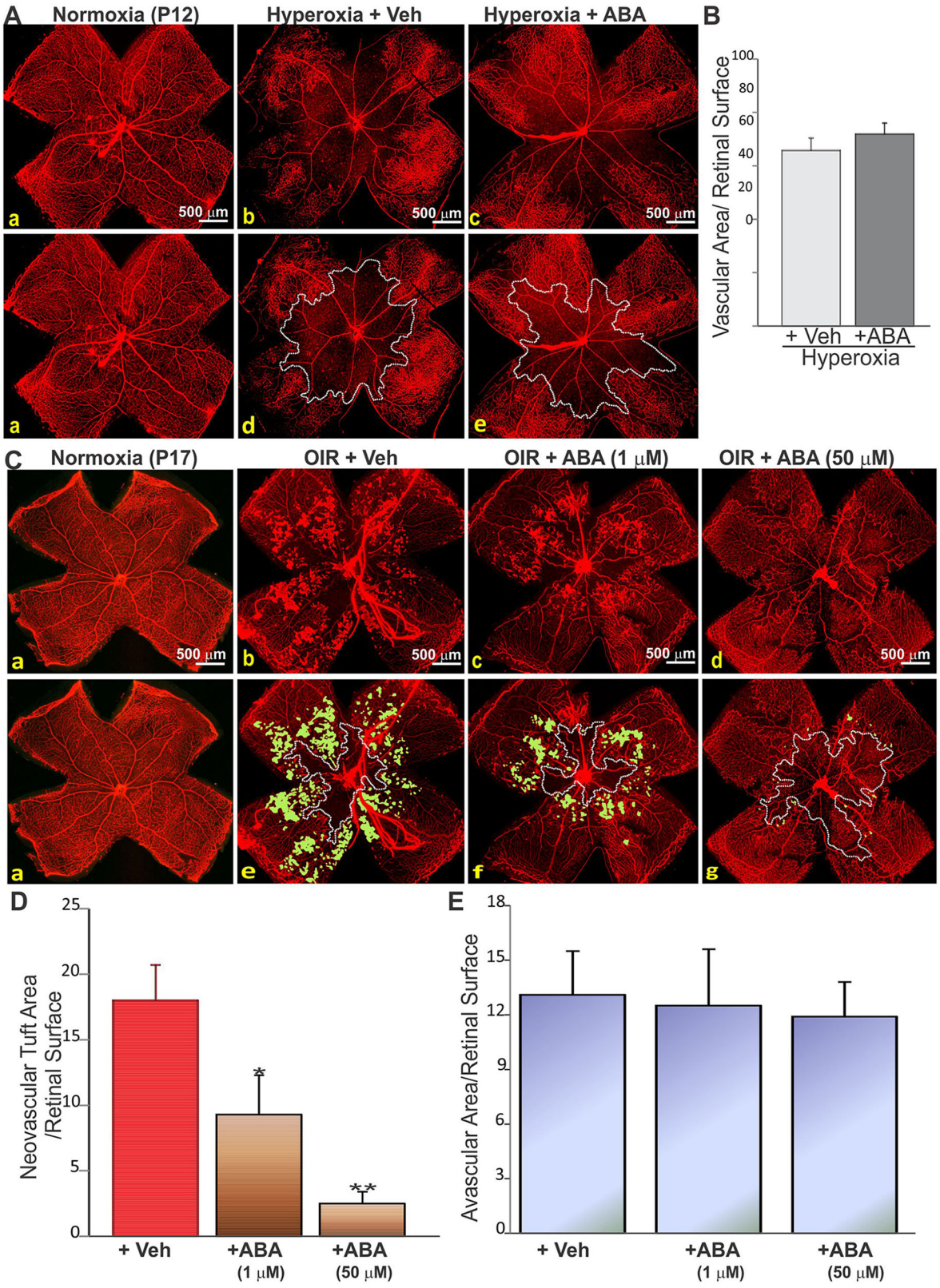

Fig. 4. Effects of ABA on hyperoxia-induced retinal vasoobliteration and preretinal neovascularization following OIR. (A) Representative flat mount preparations of IB4-stained retinas eyes at P12 from mice exposed to room air (a) or hyperoxia (75% oxygen) from P7 to P12 (b–e). OIR mice were injected intravitreally with either ABA (1 µM or 50 µM) or the vehicle alone at P6. Areas of vasoobliteration as determined by computer-assisted image analysis are delineated with dotted lines (d for b, and e for c). (B) Retinal vascular areas were normalized to the total retinal areas in P12 mice following vehicle or ABA injection. (n=6). Results are mean±s.e.m. (C) Local neovascularization in mouse retinas at P17 from mice injected with Veh or ABA and subjected to OIR. P17 mouse retinas from control normoxic mice are shown in a. Areas of vasoobliteration and preretinal neovasular tuft formation are shown in white and green, respectively (e for b, f for c, and g for d). (D,E) Compiled data (mean±s.e.m.; n=6) showing the percentage of avascular (D) and neovascular tuft areas (E) in Veh- and ABA-treated OIR mice at P17. *P<0.05, **P<0.001 versus +Veh.

Journal of Cell Science (2018) 131, jcs210492. doi:10.1242/jcs.210492

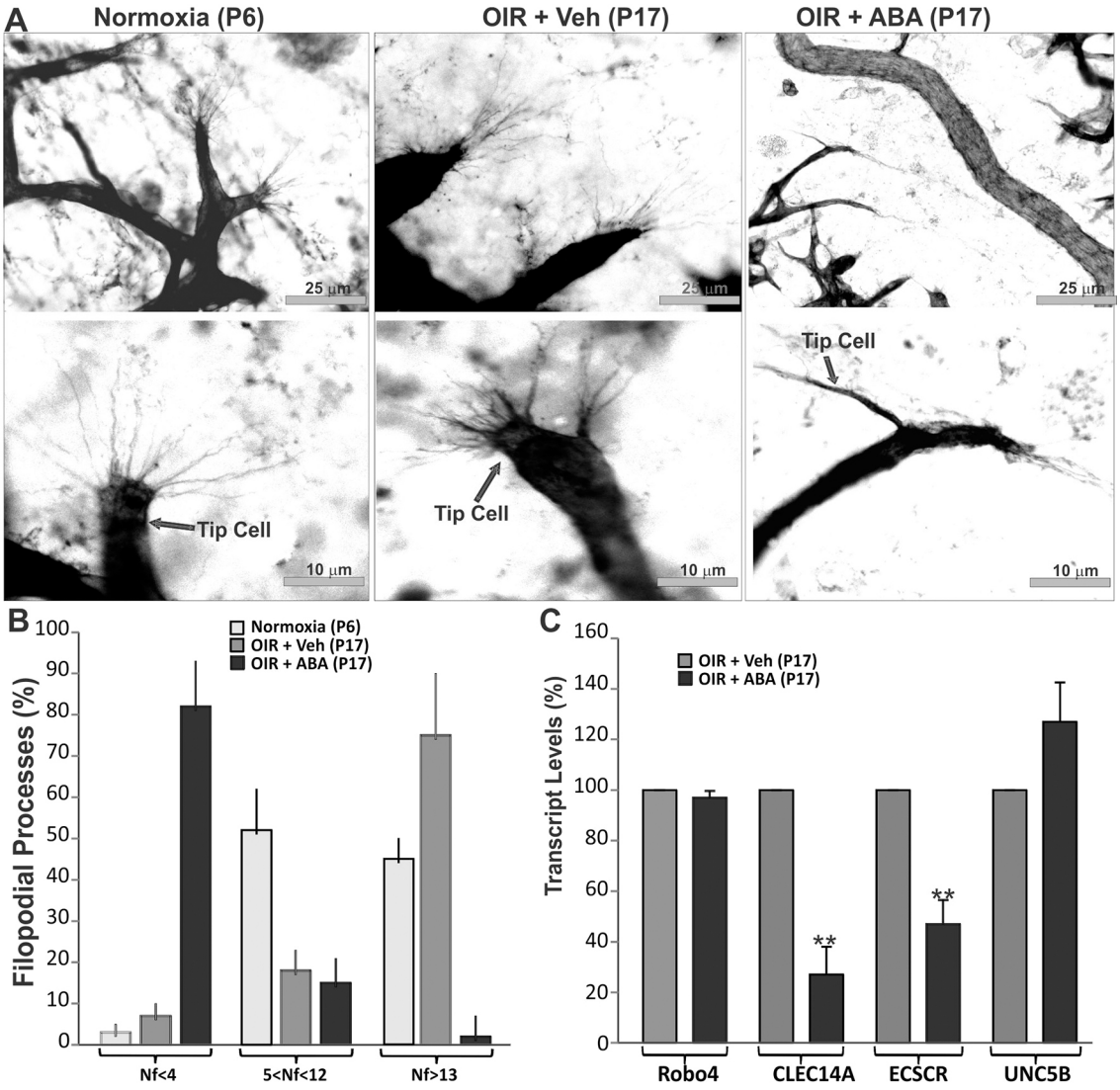

Fig. 5. Effects of ABA inhibit angiogenesis by reducing EC migratory features. (A) IB4-stained flat retinal mounts showing morphological details of tip ECs of the vascular front following OIR. Mice were either left untreated and their retinas collected at P6, or intravitreally injected with vehicle (Veh) or ABA at P13. (B) The number of filopodia (Nf) from 25 tip ECs in three different retinal preparations were counted. The mean±s.e.m. percentage of cells in each of the categories Nf<4, 5<Nf<12 and Nf>13 are shown. ***P*<0.05. (C) Expression pattern of EC-specific migratory genes in retinas from OIR mouse eyes treated with ABA or vehicle. Mice were injected with Veh or ABA at P13 following hyoeroxia and retinas were harvested at P17. The mRNA levels were normalized to those of 18 S rRNA. Data are means±s.e.m. (*n*=4). ***P*<0.05 versus OIR+Veh (P17).

the tissue. The expression of Socs3 was highly increased following ABA treatment even though Socs3-positive macrophages are associated with an M2-like macrophage phenotype (Nakamura et al., 2015). Thus, although ABA treatment did not lead to an all-or-nothing macrophage polarization response, it largely promoted an anti-angiogenic (M1) polarization state of macrophages.

ABA accelerates macrophage-dependent fetal hyaloid vessel regression

Macrophages rapidly recognize and engulf dead cells, a process that prevents the expression and release of inflammatory and angiogenic intracellular components (Savill, 1992). This process is particularly amplified during vascular remodeling associated with programmed regression of the fetal vasculature. In the mouse eye, macrophages are largely responsible for inducing the regression of fetal blood vessels that include the pupillary membrane, tunica vasculosa lentis and hyaloid vessels (HVs). Accordingly, we hypothesized that ABA treatment will enhance fetal vessel regression by virtue of its ability to skew macrophage polarization towards anti-angiogenic phenotypes. We tested this hypothesis by injecting mouse pups intravitreally with ABA at P4 and assessing HV regression at P6. As shown in Fig. 7A, ABA-treated eyes showed a dramatic acceleration of vessel regression. The total vascular area over a P3–P6 time course was significantly decreased in ABA- versus vehicle-treated eyes (Fig. 7B). Real-time quantitative PCR-based mRNA expression results showed a significant decrease in the amount of survival factors for ECs (e.g. VEGF) and an increase in anti-angiogenic M1 markers (e.g. Klf2 and Socs2) in ABA- versus vehicle-treated eyes (Fig. 7C). ABA treatment did not affect other growth factors such as Wnt7b and proapoptotic factors such as Ang2 (Fig. S4A,B), both of which have been suggested to promote withdrawal of survival factors from ECs (Kurihara et al., 2010). The anti-angiogenic properties of ABA are consistent with its ability to suppress angiogenesis and enhance the physiological involution of

Journal of Cell Science (2018) 131, jcs210492. doi:10.1242/jcs.210492

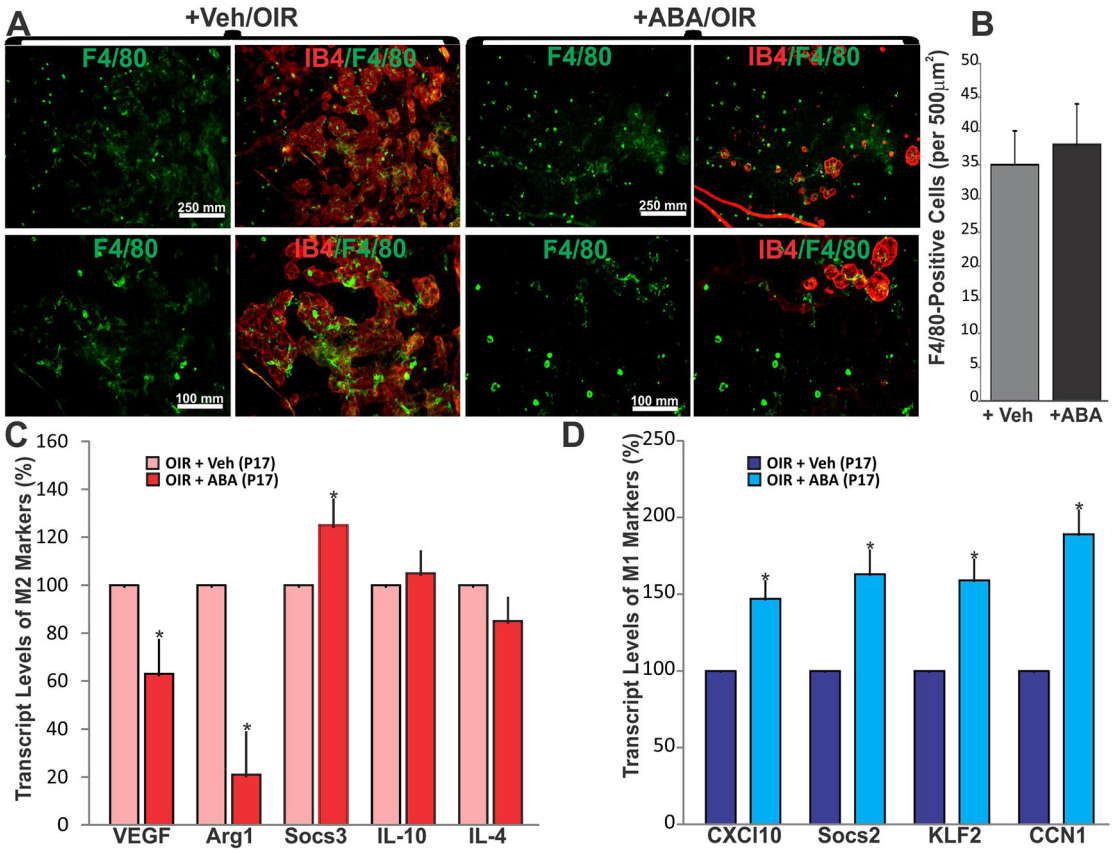

Fig. 6. ABA dampened retinal neovascularization by skewing macrophage polarization towards the M1 phenotype. (A) Type VI collagen- and/or F4/80-stained retinal flat mounts from OIR mice injected at P13 with either a vehicle or ABA and harvested at P17. Note the presence of macrophages in both avascular and neovascular areas of the retinas in both ABA- and Veh-treated eyes. (B) Percentage of F4/80-positive macrophages infiltrated in OIR retinas following injection of Veh or ABA. The number of macrophages was normalized to retinal area. (C-D) Quantification of M1 and M2 markers of macrophage polarization in retinal lysates following treatment with either Veh or ABA as determined by qPCR. Transcripts levels in Veh-treated eyes were set to 100% to facilitate comparisons among animals. **P*<0.05 versus +Veh (*n*=6).

fetal blood vessels. Therefore, not only does ABA interfere with aberrant tissue vascularization, but it also appears to suppress abnormal persistence of fetal vessels, a characteristic feature of HV persistence syndrome in humans.

DISCUSSION

ABA is a vital phytohormone which, despite its name, does not control abscission directly. The presence of ABA in abscising organs reflects its role in promoting processes that precede abscission, such as senescence, and the stress response or adaptation. When stress signals increase, plants produce excessive levels of ABA, and when stress signals are attenuated, ABA is rapidly degraded into inactive metabolites (Černý et al., 2016).

Since ABA is present in vegetables and fruits, dietary intake may provide a significant source of ABA in humans. In accordance with this, ABA has been shown to play an important role in managing glucose homeostasis and exhibiting anti-tumorigenic effects in humans, suggesting that ABA activity is therapeutically relevant in pathological processes affecting vertebrates (Zocchi et al., 2017). Herein, we demonstrate, for the first time, the preclinical effectiveness and potential usefulness of ABA as an anti-angiogenic agent. Using both *in vitro* angiogenesis assays and the retina model of physiological angiogenesis in newborn mice, we showed that ABA treatment blocked key steps in the initiation of sprouting angiogenesis including EC differentiation, migration and proliferation. ABA dose-dependently inhibited EC sprouting without affecting cell viability at doses of up to 50 µM. Even micromolar concentrations of ABA retained anti-angiogenic properties both *in vitro* and *in vivo*. During postnatal retinal vascular development, ABA induced a marked reduction of vascular density especially in the distal region of the growing vascular front where migrating tip cells and proliferating stalk cells are abundant. ABA altered endothelial tip cell number and morphology, including the abundance and dynamicity of their filopodial projections, which detect cues in the local environment and translate them into directed motility. Simultaneously, ABA reduced the proliferation rate of the trailing stalk cells (i.e. BrdU-positive cells) suggesting that ABA does not cause the premature differentiation of tip cells into stalk cells. ABA treatment increased the levels of the Notch ligand Dll4 in the leading cells, which dramatically affected the establishment of tip and stalk cell identities, and stunted vascular development.

The clinical significance of these observations was investigated in the OIR model of vasoproliferative diseases. The rodent model of OIR mimics the pathological characteristics of ROP and PDR in humans, because it recapitulates a consistent and reproducible, although aberrant, angiogenic response. Exposure of mouse pups to hyperoxia leads to the excessive regression of capillaries, while arteries become refractory to this insult (Benjamin et al., 1998). In addition to preventing new vessel growth, hyperoxia suppresses VEGF production and leads to the obliteration of already formed vessels through apoptosis (Stone et al., 1995). This suggests that

Journal of Cell Science (2018) 131, jcs210492. doi:10.1242/jcs.210492

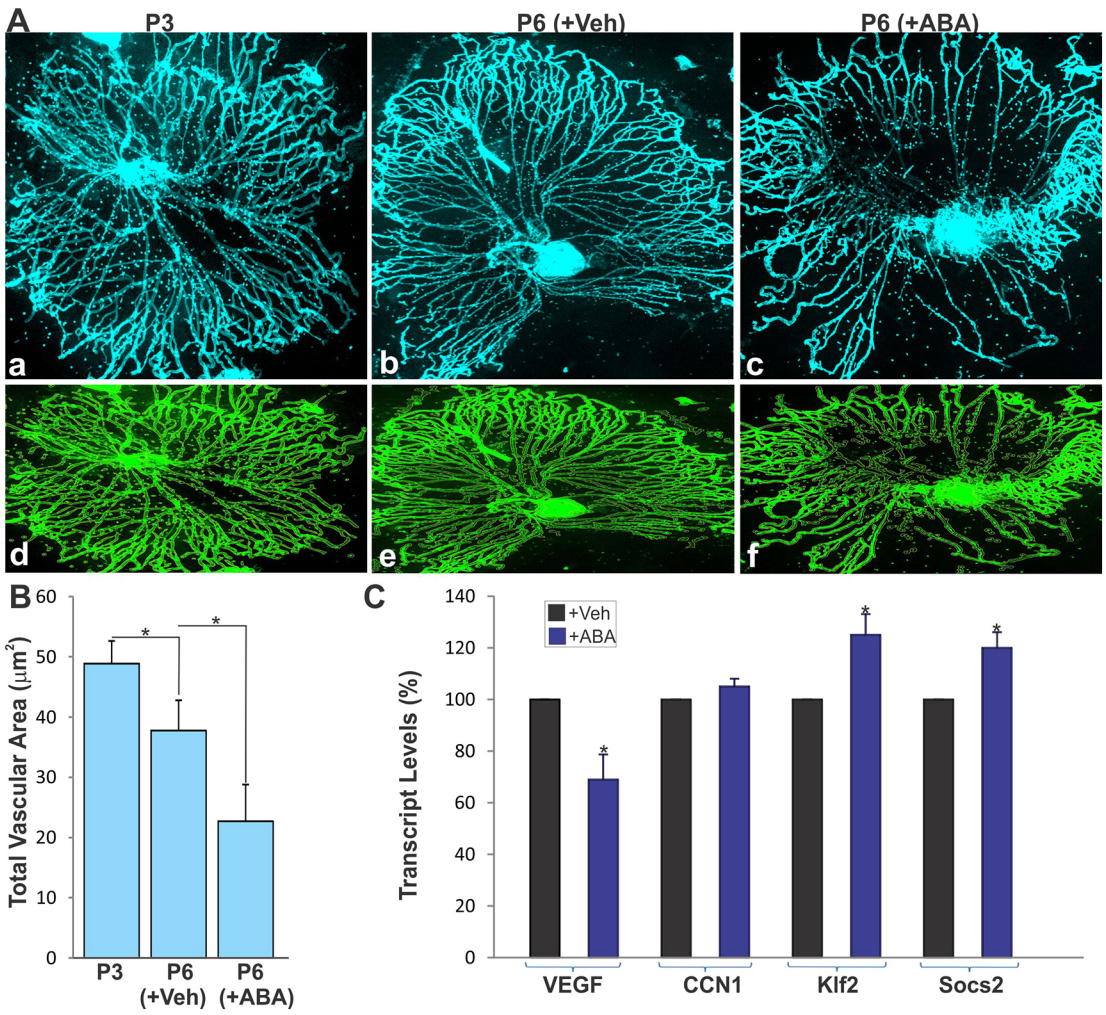

Fig. 7. ABA accelerates macrophage-dependent fetal HV regression. (A) IB4-stained preparations of HVs at postnatal days P3 and P6 after injection of either ABA or Veh at P3. Outline of HVs is shown in yellow and the vascular area is shown in green (d, e and f for a, b and c, respectively). (B) Total vascular areas as determined by Angiotool software. Mean±s.e.m. (n=6). *P<0.05. (C) Quantification of EC survival factors (e.g. VEGF, CCN1) and macrophage polarization markers (e.g. Klf2, Socs2) in the HV preparations following treatment with either Veh or ABA as determined by qPCR. Transcript levels in Veh-treated eyes were set to 100% to facilitate comparisons among HV preparations from different animals. *P<0.05 versus +Veh (n=5).

vascular pruning accompanying natural remodeling is caused by hyperoxia upon the onset of flow through the newly formed vascular system. Upon returning to normoxic conditions, the metabolic requirements of the retina increase concomitantly with VEGF levels, which stimulate abnormal blood vessel formation (Chaqour, 2016). In humans, this retinopathy response culminates into aggressive neovascularization, retinal detachment and vision loss (Hartnett and Lane, 2013). Therefore, OIR has become important for studying the disease mechanisms and potential treatments options for ischemic retinopathies. In this model, a single intravitreal injection of ABA significantly inhibited aberrant growth of blood vessels without inducing retinal stress, as demonstrated by unaltered GFAP expression. These effects are consistent with the function of ABA in seed dormancy during which a negative correlation between the tissue content of ABA and transcript levels of cell cycle and growth factor genes was found (Vergara et al., 2017). Given that cells are more sensitive to death stimuli when they are actively cycling, the effect of ABA culminates in desensitization of cells to mitogenic stimuli.

The anti-angiogenic effect of ABA is highly significant compared to the potency of several natural compounds that have been tested in the OIR model. In particular, genistein, resveratrol, honokiol and combretastatin A4 have been reported to be equally potent in reducing OIR-associated retinal neovascularization although they were effective only after multiple systemic injections (Griggs et al., 2002; Kim and Suh, 2010; Vavilala et al., 2013). Conversely, a single injection of ABA was sufficient to suppress neovascular growth. ABA triggered the shut-off of aberrant angiogenic ‘ON’ signals (e.g. VEGF and CTGF) and induced the active engagement of angiogenic ‘OFF’ signals which may explain its high anti-angiogenic potency. ABA targeted numerous markers of tip-stalk cell differentiation by downregulating the expression of CLEC14A and ECSCR during retinal neovascularization. Suppression of CLEC14A has been shown to dramatically reduce migration, filopodia formation and tubulogenesis of ECs, whereas the ectopic expression of CLEC14A induced strong filopodia formation (Zhuang et al., 2011). In accordance with this, mice deficient in CLEC14A display altered angiogenic sprouting and formation of severely hemorrhagic nonfunctional blood vessels (Lee et al., 2017b). Thus, ABA treatment recapitulates, at least in part, the loss of CLEC14A function. This finding is of particular clinical significance because it

Journal of Cell Science (2018) 131, jcs210492. doi:10.1242/jcs.210492

has been reported that CLEC14A expression is significantly higher in the blood vessels of solid tumors than in those of adjacent normal tissue (Mura et al., 2012), as well as in circulating ECs of cancer patients (Zanivan et al., 2013). Likewise, ABA treatment downregulated the expression of ECSCR, another endothelial tip-cell-specific protein. ECSCR promotes filopodia formation, tip cell migration and anastomosis of vascular sprouts to form new circuits through direct physical interaction with cytoskeletal proteins such as filamin A (Armstrong et al., 2008). Thus, ABA targets genes that turn quiescent ECs into active migratory tip cells or proliferating stalk cells. Interestingly, a study by Kilari et al. has shown that ECSCR knockdown inhibits VEGF-induced proliferation and markedly reduces tyrosine phosphorylation of VEGF receptor 2 (VEGFR-2) (Kilari et al., 2013), while another study by Lee et al. has shown that the blockade of VEGFR-2 signaling suppresses vascular abnormalities in tumor-bearing CLEC14A-knockout mice (Lee et al., 2017b). Thus, the activities of the CLEC14A and ECSCR gene products are intertwined with VEGF signaling. Taken together, our findings suggest that ABA suppresses vascular and neovascular growth by altering the expression of a network of functionally related genes regulating the phenotypical plasticity of ECs. A genome-wide transcriptomic analysis will be needed to identify the entire spectrum of genes and characterize their functional interactions to define the 'anti-angiogenic gene signature' associated with ABA.

Another interesting outcome of our study is that ABA modulates angiogenesis by altering the polarization state of macrophages. Macrophages are key accessory cells which develop a classic anti-angiogenic (M1) or proangiogenic (M2) phenotype in a context-dependent manner. The pathogenesis of vasoproliferative diseases has been associated with dynamic changes in macrophage activation, with classically activated M1 cells involved in the resolution and 'smoldering' of angiogenesis, and M2 or M2-like cells implicated in initiating and sustaining angiogenesis (Suzuki et al., 2012). Functional skewing of macrophages occurs *in vivo* under hypoxic or inflammatory conditions (Marchetti et al., 2011). However, the coexistence of cells in different activation states or mixed phenotypes has also been observed due to the complexity and dynamicity of tissue-derived signals (Amit et al., 2016). Both M1- and M2-like macrophages have been shown to be present in OIR retinas, although M2 macrophages were four times more abundant than M1 macrophages (Gao et al., 2017). The 'ON' and 'OFF' expression of a network of transcription factors and genes may account for the different states of macrophage activation (Porta et al., 2015). Our data showed that ABA skewed the polarized activation of macrophages to the M1 phenotype, which contributed to suppression of neovascularization. Although the intravitreal injection of ABA in OIR mice did not significantly affect macrophage recruitment to the ischemic retina, the expression of selective M2 markers (e.g. Arg1 and IL-4) was decreased whereas the expression of M1 markers (e.g. CXCl10, Socs 2, KLF2 and CCN1) was increased. Of note, we can only perform a limited analysis of *in vivo* M2 genes because the M1- and M2-specific gene signatures defined *in vitro* are highly influenced by important *in vivo* factors that are not necessarily recapitulated *in vitro*.

ABA-induced skewing of the macrophage phenotype was further ascertained in the mouse model of fetal vascular regression. The programmed regression of the fetal hyaloid vasculature is a simple and easy model to test the effects of ABA on macrophage–EC crosstalk *in vivo*. Macrophages drive the most critical aspects of fetal vessel regression as previously evidenced by the persistence of these vessels in macrophage-depleted mice (Lang and Bishop, 1993). ABA-treated eyes displayed advanced involution of hyaloid vessels in the central and middle region near the optic nerve. The total vascular area was significantly reduced and EC proliferation in hyaloid vessels was conspicuously low in ABA-treated eyes. In agreement with this, HVs treated with ABA expressed a reduced amount of proangiogenic factors including Klf2, Socs2 and VEGF. Concomitantly, most angiogenic marker levels were reduced or undetectable. Thus, ABA promotes a non-canonical pathway of vessel involution by amplifying macrophage-derived signals that suppress endothelial growth and survival.

Our findings reveal a novel anti-angiogenic function of ABA and provide the preclinical basis for the potential usefulness of this phytohormone for treatment of neovascular eye diseases affecting humans. Our study also identified important cellular and molecular pathways whereby ABA curtails inflammation and benign neovascular growth. Further studies of ABA-based signal transduction pathways at the membrane and nuclear levels will be needed to translate our findings into meaningful therapeutic advances. ABA has recently received increased attention due to its PPAR coactivating and anti-inflammatory properties (Guri et al., 2008). ABA treatment has been reported to activate PPARγ in macrophages through adenylate cyclase–cAMP signaling (Bassaganya-Riera et al., 2011). In addition, ABA significantly decreased the levels of other inflammatory mediators including MCP-1 and IL-6, which, in turn, reduced systemic inflammation. Potentially, ABA shares selective anti-inflammatory mechanisms with those of anti-inflammatory chemicals. Taken together with our data, these observations indicate that ABA is naturally optimized to interfere with neovascular growth by not only regulating the differentiation state of ECs but also by harnessing local vascular inflammation in the tissue target. Further studies are needed to determine how the ABA signals are transduced to and integrated with downstream angiogenic and anti-angiogenic signaling pathways in both vascular and inflammatory cells.

MATERIALS AND METHODS

Reagents

ABA was purchased from Sigma (St Louis, MO; 90769) and was dissolved in 100% United States Pharmacopeia (USP) grade DMSO. The final DMSO concentration in cell culture did not exceed 0.1% throughout the study. All other chemicals used were of reagent grade.

Cell culture

Retinal ECs were obtained from Cellpro (San Pedro, CA). The EC phenotype was validated through several criteria: (1) 'cobblestone' morphology appearance, (2) positive staining for Factors VIII, (3) uptake of acetylated low-density lipoprotein, and (4) CD-31 and IB4 positivity. Cell were maintained in Dulbecco's modified Eagle's medium (DMEM) supplemented with fetal bovine serum (FBS) glutamine and antibiotics. Cells were tested and proven to be free of contamination.

Fibrin-bead-based angiogenesis and migration assays

Cultured ECs were mixed with dextran-coated Cytodex 3 microcarrier (MC) beads (GE Healthcare Life Sciences) and incubated overnight in FBS-containing medium. For analysis of 3D sprout formation, cell-laden beads were incorporated within fibrin gels as previously described with minor modifications (Lee et al., 2017a). Briefly, beads were re-suspended in fibrinogen (Sigma) solution (4 mg/ml in 0.9% NaCl) supplemented with aprotinin (Sigma; ∼60 µg/ml) and thrombin [Sigma; 2.1 U/ml in phosphate-buffered saline (PBS)], which were added at a 4:5 ratio, and allowed to clot in 24-well tissue culture plates. A fibroblast feeder layer was added on top of the fibrin gel. The medium was changed regularly with new addition of the indicated reagent. EC sprouting was monitored after 3 and 6 days, and scored for filopodia, angiogenic sprouts and dissociated ECs. A sprout was

defined as an EC migrating outwards linearly while remaining interconnected with other cells anchored to the bead. Representative images of sprout formation were taken at different magnifications using an inverted Olympus microscope.

Trypan Blue exclusion assay

EC-coated beads (1×10^5/well) embedded in fibrinogen–thrombin gel were cultured for 3 days and exposed in 96-well plates to Trypan Blue for 2 min. Afterwards, cells were washed with PBS and then microscopically examined to determine whether cells did or did not exclude the dye. Viable cells have a clear cytoplasm whereas nonviable cells have a blue cytoplasm.

TUNEL staining

TUNEL staining was performed with the ApopTag Fluorescein *in situ* apoptosis detection kit (S7110; EMD Millipore, Billerica, MA) according to the manufacturer's protocol. TUNEL-positive nuclei were counted and normalized to the number of DAPI-positive nuclei.

OIR

Animal studies were carried out in accordance with the recommendations in the Guide for the Care and Use of Laboratory Animals of the National Institutes of Health. The protocol was approved by the Committee on the Ethics of Animal Experiments of the State University of New York-Downstate Medical Center. Ischemic retinopathy was induced in male and female C57BL/6J mice as previously described (Yan et al., 2015). Neonatal mice and their nursing dams were exposed to 75% oxygen in a PRO-OX 110 chamber oxygen controller from Biospherix Ltd (Redfield, NY) between postnatal day 7 (P7) and P12 producing vaso-obliteration and cessation of vascular development in the capillary beds of the central retina. On P12, the mice were placed in room air until P17 when the retinas were assessed for maximum neovascular response. Mice were exposed to 12-h cyclical broad spectrum light. The room temperature was maintained at 28°C.

For developmental studies, mice were raised in room air under standard light and temperature conditions. Mice were euthanized at the indicated time periods after birth by means of CO_2 euthanasia and cervical dislocation, or by decapitation. Eyes were enucleated and processed for histological and molecular analyses as described in the text.

Intravitreal injection of ABA

Mice were anesthetized by light cryo-anesthesia. ABA (50 µM) was injected intravitreally at P14 using a 33-gauge needle. In the contralateral eye, an equal volume of vehicle (DMSO) alone was injected. Retinas were dissected and processed for molecular and immunohistochemical analyses as described in the text.

HV preparation and analysis of vascular regression

Animals were euthanized and their eyeballs were enucleated and fixed in 4% paraformaldehyde (PFA) in PBS for 30 min. Eyes were injected with a 1.5% solution of low-melting-point agarose in PBS and kept at 4°C for 24 h. The HVs embedded in agarose were removed from the retinal cup, and the agarose was carefully removed using tweezers. The HV preparations were placed on a slightly heated glass slide to remove residual agarose around the HVs. The preparations were then permeabilized with 0.05% Triton X-100 in PBS and processed for immunohistochemical analyses. Vascular parameters were measured by using the AngioTool software (Zudaire et al., 2011). By assessing the variation in foreground and background pixel mass densities across an image, the software determines morphological and spatial parameters, including the overall size of the vascular network, the total and average vessel length, and vessel junctional density. Four fluorescent images were taken from four mice. The data are presented as means±s.e.m. The statistical significance of differences among mean values was determined by means of one-way analysis of variance and two-tailed *t*-test.

BrdU incorporation assay

BrdU was administered at 10 mg/kg intraperitoneally at P5. For BrdU labeling, retinas were digested with Proteinase K (10 µg/ml), fixed in 4% PFA, treated with DNase I (0.1 units/ml) for 2 h at 37°C, and incubated with anti-BrdU antibody (BD Pharmingen, dilution 1:50). ECs were visualized by staining with IB4 (Molecular Probes, A568, dilution 1:50), and BrdU was detected by using directly conjugated mouse anti-BrdU–Alexa-Fluor-488 (Molecular Probes, 1:200 dilution). The number of BrdU-positive cells per surface unit in equivalent areas of retinas from control and experimental mice was determined.

Immunohistochemical and TUNEL staining and quantification of retinal vasculature

Retinas were dissected, laid flat on SuperFrost® Plus coated slides and permeabilized in 0.1% Triton X-100 at room temperature for 20 min. Blood vessels were visualized by IB4 staining as previously described (Chintala et al., 2015). Immunostaining with primary antibodies was performed overnight at 4°C. The following day, retinas were washed three times for 5 min each in PBS and incubated with a secondary antibody overnight at 4°C. The following primary and secondary antibodies were used: goat anti-Dll4 (R&D Systems, AF1389, 1:50 dilution), rabbit anti-rat F4/80 (Bio-Rad, MCA497GA, 1:200 dilution); Alex Fluor 594-conjugated donkey anti-goat-IgG (Invitrogen, A11058, dilution 1:500) and Alexa Fluor 594-conjugated goat anti-rat IgG (Invitrogen, A11007, 1:500 dilution). Retinas were mounted in a Vectashield mounting medium (Vector Laboratories, Burlingame, CA) and images were captured using a Leica DM5000 B fluorescence microscope. Fields of view of the retinal vascular networks were captured using 2× and 40× objective lenses and included regions of capillary-sized vessels directly adjacent to radial arterioles. The areas of vasoobliteration were measured by delineating the avascular zone in the central retina and calculating the total area using Photoshop CS5 (Adobe). Similarly, the areas of pre-retinal neovascularization (i.e. neovascular tufts) were calculated by selecting regions containing tufts, which appear more brightly stained than the normal vasculature based on pixel intensities (Hasan et al., 2011). Selected regions were then summed to generate a total area of neovascularization. The avascular and neovascular areas were expressed as a percentage of the total retinal area.

For the TUNEL assay, enucleated and paraformaldehyde-fixed eyes were incubated overnight in sucrose solution. Eyes was frozen in Tissue-Tek Optimal Cutting Temperature compound, and 10-µm-thick cryostat sections were prepared. Cross-sections were then permeabilized in 0.1% Triton X-100 at room temperature for 20 min. TUNEL staining was performed with a ApopTag Fluorescein In Situ Apoptosis Detection Kit and sections were counterstained with IB4. TUNEL-positive cells in the retina were counted and adjusted to the numbers of cells per 200 μm^2 of the ONL.

RNA isolation and quantitative analysis of mRNAs

Total RNA was extracted from either cells or tissues by using an RNAEasy column purification protocol (Qiagen) according to the manufacturer's instructions. Steady-state levels of specific mRNAs were determined by real-time quantitative PCR (qPCR) using TaqMan technology on a StepOne ABI sequence detection system (Applied Biosystems, Carlsbad, CA). Highly specific primers were designed using Web-based primer design programs. The cycling parameters for qPCR amplification reactions were: AmpliTaq activation at 95°C for 10 min, denaturation at 95°C for 15 s, and annealing/extension at 60°C for 1 min (40 cycles). Triplicate *Ct* values were analyzed with Microsoft Excel by using the comparative *Ct* ($\Delta\Delta^{Ct}$) method as described by the manufacturer. The transcript amount ($-2^{\Delta\Delta Ct}$) was obtained by normalizing to an endogenous reference (18S rRNA) relative to a calibrator.

Statistical analysis

Data were expressed as mean values and standard error of mean (s.e.m.). For OIR studies, consistent mouse weights from the same size litters were used when making comparisons between or among groups because postnatal weight gain and litter size are independent factors in OIR (Vanhaesebrouck et al., 2009). Furthermore, analyses were performed on preparations where researchers were blind to the experimental condition. The SWIFT-NV method was used to minimize inter-user variability and user bias when measuring the extent of neovascularization (Stahl et al., 2009). A one-way ANOVA with a Newman–Keuls multiple comparison test was used to test differences among mean values from different groups for significance.

Where appropriate, a post hoc unpaired *t*-test was used to compare two means/groups (e.g. +vehicle or +ABA), and $P<0.05$ or $P<0.01$ was considered significant. Statistical analyses were performed using the Prism software for Windows (GraphPad Inc., San Diego, CA).

Acknowledgements
The authors would like to thank past and present laboratory members for their assistance, helpful discussion and critical comments on the manuscript.

Competing interests
The authors declare no competing or financial interests.

Author contributions
Conceptualization: J.C.; Methodology: J.C., S.L., B.C.; Software: J.C.; Validation: J.C., S.L., A.R.; Formal analysis: S.L., A.R., B.C.; Investigation: J.C., S.L., A.R.; Data curation: S.L., A.R.; Writing - original draft: B.C.; Writing - review & editing: B.C.; Supervision: S.L., B.C.; Project administration: B.C.; Funding acquisition: B.C.

Funding
This work was supported in part by grants from the National Eye Institute of the National Institutes of Health (EY022091-05A1 and EY024998-01A1 to B.C.) and funds from the Research Foundation of the State University of New York. Deposited in PMC for release after 12 months.

Supplementary information
Supplementary information available online at
http://jcs.biologists.org/lookup/doi/10.1242/jcs.210492.supplemental

References

Amit, I., Winter, D. R. and Jung, S. (2016). The role of the local environment and epigenetics in shaping macrophage identity and their effect on tissue homeostasis. *Nat. Immunol.* **17**, 18-25.

Armstrong, L.-J., Heath, V. L., Sanderson, S., Kaur, S., Beesley, J. F. J., Herbert, J. M. J., Legg, J. A., Poulsom, R. and Bicknell, R. (2008). ECSM2, an endothelial specific filamin a binding protein that mediates chemotaxis. *Arterioscler. Thromb. Vasc. Biol.* **28**, 1640-1646.

Bassaganya-Riera, J., Guri, A. J., Lu, P., Climent, M., Carbo, A., Sobral, B. W., Horne, W. T., Lewis, S. N., Bevan, D. R. and Hontecillas, R. (2011). Abscisic acid regulates inflammation via ligand-binding domain-independent activation of peroxisome proliferator-activated receptor gamma. *J. Biol. Chem.* **286**, 2504-2516.

Battegay, E. J. (1995). Angiogenesis: mechanistic insights, neovascular diseases, and therapeutic prospects. *J. Mol. Med.* **73**, 333-346.

Benjamin, L. E., Hemo, I. and Keshet, E. (1998). A plasticity window for blood vessel remodelling is defined by pericyte coverage of the preformed endothelial network and is regulated by PDGF-B and VEGF. *Development* **125**, 1591-1598.

Brar, V. S., Sharma, R. K., Murthy, R. K. and Chalam, K. V. (2010). Bevacizumab neutralizes the protective effect of vascular endothelial growth factor on retinal ganglion cells. *Mol. Vis.* **16**, 1848-1853.

Bruzzone, S., Moreschi, I., Usai, C., Guida, L., Damonte, G., Salis, A., Scarfi, S., Millo, E., De Flora, A. and Zocchi, E. (2007). Abscisic acid is an endogenous cytokine in human granulocytes with cyclic ADP-ribose as second messenger. *Proc. Natl. Acad. Sci. USA* **104**, 5759-5764.

Bruzzone, S., Bodrato, N., Usai, C., Guida, L., Moreschi, I., Nano, R., Antonioli, B., Fruscione, F., Magnone, M., Scarfi, S. et al. (2008). Abscisic acid is an endogenous stimulator of insulin release from human pancreatic islets with cyclic ADP ribose as second messenger. *J. Biol. Chem.* **283**, 32188-32197.

Bruzzone, S., Basile, G., Mannino, E., Sturla, L., Magnone, M., Grozio, A., Salis, A., Fresia, C., Vigliarolo, T., Guida, L. et al. (2012). Autocrine abscisic acid mediates the UV-B-induced inflammatory response in human granulocytes and keratinocytes. *J. Cell. Physiol.* **227**, 2502-2510.

Černý, M., Novák, J., Habánová, H., Cerna, H. and Brzobohatý, B. (2016). Role of the proteome in phytohormonal signaling. *Biochim. Biophys. Acta* **1864**, 1003-1015.

Chaqour, B. (2013). Molecular control of vascular development by the matricellular proteins (CCN1/CYR61) and (CCN2/CTGF). *Trends Dev. Biol.* **7**, 59-72.

Chaqour, B. (2016). Regulating the regulators of angiogenesis by CCN1 and taking it up a Notch. *J. Cell Commun. Signal.* **10**, 259-261.

Chintala, H., Krupska, I., Yan, L., Lau, L., Grant, M. and Chaqour, B. (2015). The matricellular protein CCN1 controls retinal angiogenesis by targeting VEGF, Src homology 2 domain phosphatase-1 and Notch signaling. *Development* **142**, 2364-2374.

Das, A. and McGuire, P. G. (2003). Retinal and choroidal angiogenesis: pathophysiology and strategies for inhibition. *Prog. Retin. Eye Res.* **22**, 721-748.

Eremina, V., Sood, M., Haigh, J., Nagy, A., Lajoie, G., Ferrara, N., Gerber, H.-P., Kikkawa, Y., Miner, J. H. and Quaggin, S. E. (2003). Glomerular-specific alterations of VEGF-A expression lead to distinct congenital and acquired renal diseases. *J. Clin. Invest.* **111**, 707-716.

Eremina, V., Cui, S., Gerber, H., Ferrara, N., Haigh, J., Nagy, A., Ema, M., Rossant, J., Jothy, S., Miner, J. H. et al. (2006). Vascular endothelial growth factor a signaling in the podocyte-endothelial compartment is required for mesangial cell migration and survival. *J. Am. Soc. Nephrol.* **17**, 724-735.

Fujiwara, M., Ghazizadeh, M. and Kawanami, O. (2006). Potential role of the Slit/Robo signal pathway in angiogenesis. *Vasc. Med* **11**, 115-121.

Gao, S., Li, C., Zhu, Y., Wang, Y., Sui, A., Zhong, Y., Xie, B. and Shen, X. (2017). PEDF mediates pathological neovascularization by regulating macrophage recruitment and polarization in the mouse model of oxygen-induced retinopathy. *Sci. Rep.* **7**, 42846.

Griggs, J., Skepper, J. N., Smith, G. A., Brindle, K. M., Metcalfe, J. C. and Hesketh, R. (2002). Inhibition of proliferative retinopathy by the anti-vascular agent combretastatin-A4. *Am. J. Pathol.* **160**, 1097-1103.

Guri, A. J., Hontecillas, R., Ferrer, G., Casagran, O., Wankhade, U., Noble, A. M., Eizirik, D. L., Ortis, F., Cnop, M., Liu, D. et al. (2008). Loss of PPAR gamma in immune cells impairs the ability of abscisic acid to improve insulin sensitivity by suppressing monocyte chemoattractant protein-1 expression and macrophage infiltration into white adipose tissue. *J. Nutr. Biochem.* **19**, 216-228.

Hartnett, M. E. (2015). Pathophysiology and mechanisms of severe retinopathy of prematurity. *Ophthalmology* **122**, 200-210.

Hartnett, M. E. and Lane, R. H. (2013). Effects of oxygen on the development and severity of retinopathy of prematurity. *J. AAPOS* **17**, 229-234.

Hasan, A., Pokeza, N., Shaw, L., Lee, H.-S., Lazzaro, D., Chintala, H., Rosenbaum, D., Grant, M. B. and Chaqour, B. (2011). The matricellular protein cysteine-rich protein 61 (CCN1/Cyr61) enhances physiological adaptation of retinal vessels and reduces pathological neovascularization associated with ischemic retinopathy. *J. Biol. Chem.* **286**, 9542-9554.

Hellström, M., Phng, L.-K., Hofmann, J. J., Wallgard, E., Coultas, L., Lindblom, P., Alva, J., Nilsson, A.-K., Karlsson, L., Gaiano, N. et al. (2007). Dll4 signalling through Notch1 regulates formation of tip cells during angiogenesis. *Nature* **445**, 776-780.

Hontecillas, R., Roberts, P. C., Carbo, A., Vives, C., Horne, W. T., Genis, S., Velayudhan, B. and Bassaganya-Riera, J. (2013). Dietary abscisic acid ameliorates influenza-virus-associated disease and pulmonary immunopathology through a PPARgamma-dependent mechanism. *J. Nutr. Biochem.* **24**, 1019-1027.

Jacobsen, J. V., Pearce, D. W., Poole, A. T., Pharis, R. P. and Mander, L. N. (2002). Abscisic acid, phaseic acid and gibberellin contents associated with dormancy and germination in barley. *Physiol. Plant* **115**, 428-441.

Kilari, S., Remadevi, I., Zhao, B., Pan, J., Miao, R., Ramchandran, R., North, P. E., You, M., Rahimi, N. and Wilkinson, G. A. (2013). Endothelial cell-specific chemotaxis receptor (ECSCR) enhances vascular endothelial growth factor (VEGF) receptor-2/kinase insert domain receptor (KDR) activation and promotes proteolysis of internalized KDR. *J. Biol. Chem.* **288**, 10265-10274.

Kim, W. T. and Suh, E. S. (2010). Retinal protective effects of resveratrol via modulation of nitric oxide synthase on oxygen-induced retinopathy. *Korean J. Ophthalmol.* **24**, 108-118.

Kimoto, K. and Kubota, T. (2012). Anti-VEGF agents for ocular angiogenesis and vascular permeability. *J. Ophthalmol.* **2012**, 852183.

Koch, U., Fiorini, E., Benedito, R., Besseyrias, V., Schuster-Gossler, K., Pierres, M., Manley, N. R., Duarte, A., Macdonald, H. R. and Radtke, F. (2008). Delta-like 4 is the essential, nonredundant ligand for Notch1 during thymic T cell lineage commitment. *J. Exp. Med.* **205**, 2515-2523.

Krupska, I., Bruford, E. A. and Chaqour, B. (2015). Eyeing the Cyr61/CTGF/NOV (CCN) group of genes in development and diseases: highlights of their structural likenesses and functional dissimilarities. *Hum. Genomics* **9**, 24.

Kuiper, E. J., van Nieuwenhoven, F. A., de Smet, M. D., van Meurs, J. C., Tanck, M. W., Oliver, N., Klaassen, I., Van Noorden, C. J. F., Goldschmeding, R. and Schlingemann, R. O. (2008). The angio-fibrotic switch of VEGF and CTGF in proliferative diabetic retinopathy. *PLoS ONE* **3**, e2675.

Kurihara, T., Kubota, Y., Ozawa, Y., Takubo, K., Noda, K., Simon, M. C., Johnson, R. S., Suematsu, M., Tsubota, K., Ishida, S. et al. (2010). von Hippel-Lindau protein regulates transition from the fetal to the adult circulatory system in retina. *Development* **137**, 1563-1571.

Kuromori, T., Miyaji, T., Yabuuchi, H., Shimizu, H., Sugimoto, E., Kamiya, A., Moriyama, Y. and Shinozaki, K. (2010). ABC transporter AtABCG25 is involved in abscisic acid transport and responses. *Proc. Natl. Acad. Sci. USA* **107**, 2361-2366.

Lang, R. A. and Bishop, J. M. (1993). Macrophages are required for cell death and tissue remodeling in the developing mouse eye. *Cell* **74**, 453-462.

Lee, S., Elaskandrany, M., Lau, L. F., Lazzaro, D., Grant, M. B. and Chaqour, B. (2017a). Interplay between CCN1 and Wnt5a in endothelial cells and pericytes determines the angiogenic outcome in a model of ischemic retinopathy. *Sci. Rep.* **7**, 1405.

Lee, S., Rho, S.-S., Park, H., Park, J. A., Kim, J., Lee, I.-K., Koh, G. Y., Mochizuki, N., Kim, Y.-M. and Kwon, Y.-G. (2017b). Carbohydrate-binding protein CLEC14A regulates VEGFR-2- and VEGFR-3-dependent signals during angiogenesis and lymphangiogenesis. *J. Clin. Invest.* **127**, 457-471.

Marchetti, V., Yanes, O., Aguilar, E., Wang, M., Friedlander, D., Moreno, S., Storm, K., Zhan, M., Naccache, S., Nemerow, G. et al. (2011). Differential macrophage polarization promotes tissue remodeling and repair in a model of ischemic retinopathy. *Sci. Rep.* **1**, 76.

Mervin, K. and Stone, J. (2002). Developmental death of photoreceptors in the C57BL/6J mouse: association with retinal function and self-protection. *Exp. Eye Res.* **75**, 703-713.

Meshkani, R. and Vakili, S. (2016). Tissue resident macrophages: key players in the pathogenesis of type 2 diabetes and its complications. *Clin. Chim. Acta* **462**, 77-89.

Mura, M., Swain, R. K., Zhuang, X., Vorschmitt, H., Reynolds, G., Durant, S., Beesley, J. F. J., Herbert, J. M. J., Sheldon, H., Andre, M. et al. (2012). Identification and angiogenic role of the novel tumor endothelial marker CLEC14A. *Oncogene* **31**, 293-305.

Nakamura, R., Sene, A., Santeford, A., Gdoura, A., Kubota, S., Zapata, N. and Apte, R. S. (2015). IL10-driven STAT3 signalling in senescent macrophages promotes pathological eye angiogenesis. *Nat. Commun.* **6**, 7847.

Nakatsu, M. N., Sainson, R. C. A., Aoto, J. N., Taylor, K. L., Aitkenhead, M., Perez-del-Pulgar, S., Carpenter, P. M. and Hughes, C. C. W. (2003). Angiogenic sprouting and capillary lumen formation modeled by human umbilical vein endothelial cells (HUVEC) in fibrin gels: the role of fibroblasts and Angiopoietin-1. *Microvasc. Res.* **66**, 102-112.

Ng, L. M., Melcher, K., Teh, B. T. and Xu, H. E. (2014). Abscisic acid perception and signaling: structural mechanisms and applications. *Acta Pharmacol. Sin.* **35**, 567-584.

Nishijima, K., Ng, Y.-S., Zhong, L., Bradley, J., Schubert, W., Jo, N., Akita, J., Samuelsson, S. J., Robinson, G. S., Adamis, A. P. et al. (2007). Vascular endothelial growth factor-A is a survival factor for retinal neurons and a critical neuroprotectant during the adaptive response to ischemic injury. *Am. J. Pathol.* **171**, 53-67.

Pertl, L., Steinwender, G., Mayer, C., Hausberger, S., Pöschl, E.-M., Wackernagel, W., Wedrich, A., El-Shabrawi, Y. and Haas, A. (2015). A systematic review and meta-analysis on the safety of Vascular Endothelial Growth Factor (VEGF) inhibitors for the treatment of retinopathy of prematurity. *PLoS ONE* **10**, e0129383.

Porta, C., Riboldi, E., Ippolito, A. and Sica, A. (2015). Molecular and epigenetic basis of macrophage polarized activation. *Semin. Immunol.* **27**, 237-248.

Robinson, C. J. and Stringer, S. E. (2001). The splice variants of vascular endothelial growth factor (VEGF) and their receptors. *J. Cell Sci.* **114**, 853-865.

Sakthivel, P., Sharma, N., Klahn, P., Gereke, M. and Bruder, D. (2016). Abscisic acid: a phytohormone and mammalian cytokine as novel pharmacon with potential for future development into clinical applications. *Curr. Med. Chem.* **23**, 1549-1570.

Savill, J. (1992). Macrophage recognition of senescent neutrophils. *Clin. Sci. (Lond.)* **83**, 649-655.

Semeraro, F., Morescalchi, F., Duse, S., Gambicorti, E., Cancarini, A. and Costagliola, C. (2015). Pharmacokinetic and pharmacodynamic properties of anti-VEGF drugs after intravitreal injection. *Curr. Drug Metab.* **16**, 572-584.

Stahl, A., Connor, K. M., Sapieha, P., Willett, K. L., Krah, N. M., Dennison, R. J., Chen, J., Guerin, K. I. and Smith, L. E. H. (2009). Computer-aided quantification of retinal neovascularization. *Angiogenesis* **12**, 297-301.

Stewart, M. W. (2011). Aflibercept (VEGF-TRAP): the next anti-VEGF drug. *Inflamm. Allergy Drug Targets* **10**, 497-508.

Stone, J., Itin, A., Alon, T., Pe'er, J., Gnessin, H., Chan-Ling, T. and Keshet, E. (1995). Development of retinal vasculature is mediated by hypoxia-induced vascular endothelial growth factor (VEGF) expression by neuroglia. *J. Neurosci.* **15**, 4738-4747.

Suzuki, M., Tsujikawa, M., Itabe, H., Du, Z.-J., Xie, P., Matsumura, N., Fu, X., Zhang, R., Sonoda, K.-H., Hazen, S. L., et al. (2012). Chronic photo-oxidative stress and subsequent MCP-1 activation as causative factors for age-related macular degeneration. *J. Cell Sci.* **125**, 2407-2415.

Thébaud, B. and Abman, S. H. (2007). Bronchopulmonary dysplasia: where have all the vessels gone? Roles of angiogenic growth factors in chronic lung disease. *Am. J. Respir. Crit. Care. Med.* **175**, 978-985.

Tolentino, M. (2011). Systemic and ocular safety of intravitreal anti-VEGF therapies for ocular neovascular disease. *Surv. Ophthalmol.* **56**, 95-113.

Vanhaesebrouck, S., Daniëls, H., Moons, L., Vanhole, C., Carmeliet, P. and De Zegher, F. (2009). Oxygen-induced retinopathy in mice: amplification by neonatal IGF-I deficit and attenuation by IGF-I administration. *Pediatr. Res.* **65**, 307-310.

Vavilala, D. T., O'Bryhim, B. E., Ponnaluri, V. K. C., White, R. S., Radel, J., Symons, R. C. A. and Mukherji, M. (2013). Honokiol inhibits pathological retinal neovascularization in oxygen-induced retinopathy mouse model. *Biochem. Biophys. Res. Commun.* **438**, 697-702.

Vergara, R., Noriega, X., Aravena, K., Prieto, H. and Pérez, F. J. (2017). ABA represses the expression of cell cycle genes and may modulate the development of endodormancy in grapevine buds. *Front. Plant Sci.* **8**, 812.

Verma, A., Bhattacharya, R., Remadevi, I., Li, K., Pramanik, K., Samant, G. V., Horswill, M., Chun, C. Z., Zhao, B., Wang, E. et al. (2010). Endothelial cell-specific chemotaxis receptor (ecscr) promotes angioblast migration during vasculogenesis and enhances VEGF receptor sensitivity. *Blood* **115**, 4614-4622.

Yan, L. and Chaqour, B. (2013). Cysteine-rich protein 61 (CCN1) and connective tissue growth factor (CCN2) at the crosshairs of ocular neovascular and fibrovascular disease therapy. *J. Cell Commun. Signal.* **7**, 253-263.

Yan, L., Lee, S., Lazzaro, D. R., Aranda, J., Grant, M. B. and Chaqour, B. (2015). Single and compound knock-outs of MicroRNA (miRNA)-155 and its angiogenic gene target CCN1 in mice alter vascular and neovascular growth in the retina via resident microglia. *J. Biol. Chem.* **290**, 23264-23281.

Zanivan, S., Maione, F., Hein, M. Y., Hernández-Fernaud, J. R., Ostasiewicz, P., Giraudo, E. and Mann, M. (2013). SILAC-based proteomics of human primary endothelial cell morphogenesis unveils tumor angiogenic markers. *Mol. Cell. Proteomics* **12**, 3599-3611.

Zhu, S.-Y., Yu, X.-C., Wang, X.-J., Zhao, R., Li, Y., Fan, R.-C., Shang, Y., Du, S.-Y., Wang, X.-F., Wu, F.-Q. et al. (2007). Two calcium-dependent protein kinases, CPK4 and CPK11, regulate abscisic acid signal transduction in Arabidopsis. *Plant Cell* **19**, 3019-3036.

Zhuang, X., Cross, D., Heath, V. L. and Bicknell, R. (2011). Shear stress, tip cells and regulators of endothelial migration. *Biochem. Soc. Trans.* **39**, 1571-1575.

Zocchi, E., Carpaneto, A., Cerrano, C., Bavestrello, G., Giovine, M., Bruzzone, S., Guida, L., Franco, L. and Usai, C. (2001). The temperature-signaling cascade in sponges involves a heat-gated cation channel, abscisic acid, and cyclic ADP-ribose. *Proc. Natl. Acad. Sci. USA* **98**, 14859-14864.

Zocchi, E., Hontecillas, R., Leber, A., Einerhand, A., Carbo, A., Bruzzone, S., Tubau-Juni, N., Philipson, N., Zoccoli-Rodriguez, V., Sturla, L. et al. (2017). Abscisic acid: a novel nutraceutical for glycemic control. *Front. Nutr.* **4**, 24.

Zudaire, E., Gambardella, L., Kurcz, C. and Vermeren, S. (2011). A computational tool for quantitative analysis of vascular networks. *PLoS ONE* **6**, e27385.